HHS Public Access

Author manuscript

Exp Cell Res. Author manuscript; available in PMC 2024 August 01.

Published in final edited form as:

Exp Cell Res. 2023 August 01; 429(1): 113617. doi:10.1016/j.yexcr.2023.113617.

Evidence for Crosstalk between the Aryl Hydrocarbon Receptor and the Translocator Protein in Mouse Lung Epithelial Cells

Michelle M. Steidemann[a,b], **Jian Liu**[c], **Kalin Bayes**[d], **Lizbeth P. Castro**[e], **Shelagh Ferguson-Miller**[c], **John J. LaPres**[b,c,*]

[a]Department of Pharmacology and Toxicology, Michigan State University, East Lansing, MI 48824, United States

[b]Institute for Integrative Toxicology, Michigan State University, East Lansing, MI 48824, United States

[c]Department of Biochemistry and Molecular Biology, Michigan State University, East Lansing, MI 48824, United States

[d]Department of Integrative Biology, Michigan State University, East Lansing, MI 48824, United States

[e]Department of Cell and Molecular Biology, University of Texas Southwestern Medical Center, Dallas, TX 75390, United States

Abstract

Cellular homeostasis requires the use of multiple environmental sensors that can respond to a variety of endogenous and exogenous compounds. The aryl hydrocarbon receptor (AHR) is classically known as a transcription factor that induces drug metabolizing enzymes when bound to toxicants such as 2,3,7,8-tetrachlorodibenzo-ρ-dioxin (TCDD). The receptor has a growing number of putative endogenous ligands, such as tryptophan, cholesterol, and heme metabolites. Many of these compounds are also linked to the translocator protein (TSPO), an outer mitochondrial membrane protein. Given a portion of the cellular pool of the AHR has also been localized to mitochondria and the overlap in putative ligands, we tested the hypothesis that crosstalk exists between the two proteins. CRISPR/Cas9 was used to create knockouts for AHR and TSPO in a mouse lung epithelial cell line (MLE-12). WT, AHR−/−, and TSPO−/− cells were then exposed to AHR ligand (TCDD), TSPO ligand (PK11195), or both and RNA-seq was performed. More mitochondrial-related genes were altered by loss of both AHR and TSPO

*Corresponding author at: Department of Biochemistry and Molecular Biology, 603 Wilson Rd., Michigan State University, East Lansing, MI 48824, United States. lapres@msu.edu (J.J. LaPres).

Credit Authors Statement:

M.S. performed most of the experiments and wrote the manuscript. J.L. performed the kynurenine binding assay and edited the manuscript. S.F.M. provided resources, experimental planning, and manuscript editing. J.J.L provided resources, experimental design and final editing of the manuscript.

Conflict of interest statement

The authors declare that there are no conflicts of interest.

than would have been expected just by chance. Some of the genes altered included those that encode for components of the electron transport system and the mitochondrial calcium uniporter. Both proteins altered the activity of the other as AHR loss caused the increase of TSPO at both the mRNA and protein level and loss of TSPO significantly increased the expression of classic AHR battery genes after TCDD treatment. This research provides evidence that AHR and TSPO participate in similar pathways that contribute to mitochondrial homeostasis.

Keywords

Aryl hydrocarbon receptor; Mitochondrial calcium uniporter; PK11195; RNA-Sequencing; 2,3,7,8-tetrachlorodibenzo-ρ-dioxin (TCDD); Translocator protein

1. Introduction

The ability to sense environmental changes and initiate an appropriate response is required by all cells, from single-celled organisms to those making up complex organ systems. These environmental cues can take many different forms, including sunlight, oxygen, and small molecules. Small molecules can include beneficial endogenous chemicals, such as hormones, but also harmful exogenous compounds, such as pollutants. Cells, therefore, need a variety of environmental sensors that are capable of coping with a vast array of inputs. The aryl hydrocarbon receptor (AHR) is one example of a conserved metazoan ligand-activated transcription factor that responds to planar aromatic hydrocarbons. The AHR was discovered due to its ability to bind to the environmental toxicant, 2,3,7,8-tetrachlorodibenzo-ρ-dioxin (TCDD) [1]. The murine AHR was later cloned and characterized by Burbach et al. [2]. In the absence of ligand, the AHR is primarily located in the cytoplasm of the cell bound to chaperones, such as AHR interacting protein (AIP, also known as ARA9 and XAP2) [3,4,5] and a HSP90 dimer [6]. Upon ligand binding, it translocates to the nucleus where it forms a heterodimer with the aryl hydrocarbon nuclear translocator (ARNT) [7]. This heterodimer is a functional transcription factor, capable of binding DNA at specific sites within the genome termed dioxin response elements (DREs) and altering gene transcription [8]. A majority of the genes containing DREs encode for chemical/drug metabolism enzymes, such as Cytochrome P450s including CYP1A1 [9] and CYP1B1 [10].

The function of the AHR is not limited to detoxification as it has also been found to be involved in processes such as calcium homeostasis [11,12] and apoptosis [13,14], two activities that can involve mitochondria. The AHR is also directly linked to mitochondrial function, as TCDD exposure can decrease maximum cellular respiration in an AHR-dependent manner [15,16]. Although the exact mechanism by which the AHR can regulate mitochondrial processes is unknown, evidence suggests that a portion of the cellular pool of the receptor can be found within the organelle. The AHR was shown to bind mitochondria-specific proteins, co-purify with mitochondria in fractionation experiments, and localize within the intermembrane space of the organelle [17,16]. Additionally, the AHR would not be the only ligand-activated transcription factor receptor that co-localizes to mitochondria. Evidence has been collected to suggest that certain isoforms of the estrogen receptor

[18,19], glucocorticoid receptor [20,21], and thyroid receptor [22,23] can all be found in mitochondria.

The presence of a mitochondrial localized AHR (mitoAHR) suggests an endogenous need for the receptor in that organelle but that function is still unknown. One clue to mitoAHR's function stems from the list of its putative endogenous ligands, which include cholesterol [24], heme [25], and tryptophan metabolites [26,27]. Interestingly, many of these same ligands are also linked to another mitochondrial protein, the translocator protein (TSPO). TSPO is a transmembrane protein associated with the outer membrane of mitochondria and is highly conserved between species, but its endogenous function is also unclear. Originally referred to as the peripheral-type benzodiazepine receptor (PBR), because of its ability to bind diazepam outside of the central nervous system [28], TSPO has also been shown to bind cholesterol [29], porphyrins [30], and retinoic acid [29]. TSPO regulates mitochondrial calcium influx through interaction with the voltage-dependent anion channel (VDAC) [31,32]. Additionally, TSPO is involved in the mitochondrial apoptosis pathway [33,34]. Considerable overlap between putative endogenous ligands for the AHR and TSPO, as well as cellular localization to mitochondria, and involvement of both proteins in stress related responses, suggest these two proteins might participate in one or more shared signaling pathways.

The goal of this paper was to investigate the possibility of crosstalk existing between the AHR and TSPO. To accomplish this both proteins were separately knocked out using Clustered Regularly Interspaced Short Palindromic Repeats/CRISPR associated protein 9 (CRISPR/Cas9) technology in murine lung epithelial cells (MLE-12s). MLE-12 cells were chosen because lung epithelium represents a barrier that would be exposed to inhaled pollutants and MLE-12s have been shown to express both AHR and TSPO. These cells were then examined to see if either could influence the expression or activity of the other, giving evidence for overlap in cellular pathways. Understanding the nature of an interaction between AHR and TSPO might provide clues to the influence of both on mitochondrial function.

2. Materials and Methods

2.1 Kynurenine Binding Assay

The kynurenine binding affinity to wild-type Rhodobacter spheroids TSPO (RsTSPO) was measured by tryptophan fluorescence quenching assay as previously described [29]. 2.5 μM purified RsTSPO WT protein (in 20mM Tris pH 8.0, 150mM NaCl, 0.20% DM, 2mM TCEP) was titrated with increasing amounts of Kynurenine dissolved in DMSO, at room temperature. The quenching curve was measured by a fluorescence scan from 290 to 400 nm (excitation at 285 nm) on an Agilent Eclipse® fluorescence spectrometer (Agilent, Santa Clara, CA). Control experiments were also performed to evaluate the absorption and emission of ligands as well as buffers and solvents. The dissociation constant Kd was calculated by fitting the binding curve with Hill equations.

2.2 Cell Culture

Mouse lung epithelial type II cell line 12 (MLE-12) cells were grown in Dulbecco's Modified Eagle Medium: Nutrient Mixture F-12 (Thermo Fisher Scientific, Waltham, MA) supplemented with fetal bovine serum (2%, Hyclone, Fisher Scientific, Waltham, MA), Insulin-Transferrin-Sodium selenite liquid media supplement (1.0 mg/ml-0.55 mg/ml-0.5 μg/ml, Sigma-Aldrich, St. Louis, MO), hydrocortisone (10 nM, Sigma-Aldrich, St. Louis, MO), β-estradiol (10 nM, Sigma-Aldrich, St. Louis, MO), HEPES (10 mM, Sigma-Aldrich, St. Louis, MO), L-glutamine (2 mM, Thermo Fisher Scientific, Waltham, MA), and penicillin/streptomycin (100 units/mL penicillin, 100 μg/mL of streptomycin, Thermo Fisher Scientific, Waltham, MA). Mouse hepatoma cell line (Hepa1c1c7) were grown in Dulbecco's Modified Eagle Medium (Thermo Fisher Scientific, Waltham, MA) supplemented with Cosmic Calf Serum (8.9%, Hyclone, Fisher Scientific, Waltham, MA), penicillin/streptomycin (100 units/mL penicillin, 100 μg/mL of streptomycin, Thermo Fisher Scientific, Waltham, MA), and MEM sodium pyruvate solution (0.89 mM, Atlanta, Flowery Branch, GA). Cells were grown in a NAPCO 8000 incubator (Thermo Fisher Scientific, Waltham, MA) at 37°C and 5% CO_2.

2.3 Knockout Cell Generation

The genes coding for AHR and TSPO were knocked out in Hepa1c1c7 and MLE-12 cells using CRISPR/Cas9 protocol based on Ran et al. [35]. Guide oligos were ligated into pSpCas9 (BB)-AA-Puro.

Guide oligo primers for *Ahr* 1.4 were:

Forward 5'-CACCGGGCGCGGGCACCATGAGCAG-3'

Reverse 5'-AAACCTGCTCATGGTGCCCGCGCCC-3'.

Guide oligo primers for *Tspo* 1.1 were:

Forward 5'-AAACCCGGTGGTATGCTAGCTTGCC-3'

Reverse 5'-CACCGGCAAGCTAGCATACCACCGG-3'

Guide oligo primers for *Tspo* 2.2 were:

Forward 5'- AAACCCTCGCTGGACACTGGCTCCC-3'

Reverse 5'- CACCGGGAGCCAGTGTCCAGCGAGG-3'

Plasmids were transfected into Hepa1c1c7 and MLE-12 cells using Lipofectamine 2000 (Thermo Fisher Scientific, Waltham, MA) based on manufacturer's protocol. Potential knockout cells were selected using puromycin (5 μg/ml). After three days cells were diluted to a density of one cell per well in a 96-well dish and then clonally expanded. Gene knockout was first confirmed through western blotting.

2.4 Western Blotting

Whole cells were collected in RIPA lysis buffer (50 mM Tris-HCl, 150 mM NaCl, 1% Igepal, 1mM EDTA, 0.25% Na-deoxycholate) supplemented with cOmplete™, Mini Protease Inhibitor Cocktail (Sigma-Aldrich, St. Louis, MO). Protein concentration

was determined using a Bradford Assay protocol with Pierce Detergent Compatible Bradford Assay Reagent (Thermo Fisher Scientific, Waltham, MA) and bovine serum albumin standards (Sigma-Aldrich, St. Louis, MO). Absorbance was read at 595 nm using SpectraMax ABS Plus (Molecular Devices, LLC, San Jose, CA). Using those concentrations, 150 μg of total whole cell protein for TSPO and 200 μg for AHR (MLE-12), and 37.5 μg for AHR (Hepa1c1c7) was loaded into each well for each of the cell lines. Proteins were separated on a 15% sodium dodecyl sulfate−polyacrylamide gel for TSPO and an 8% gel for AHR. Proteins were transferred to Amersham Protran 0.2 NC nitrocellulose membrane (GE Healthcare Life Sciences, Chicago, IL) using Trans-Blot Semi-Dry Transfer Cell (Bio-Rad Laboratories, Hercules, CA). The membranes were stained with the following primary antibodies: rabbit polyclonal anti-AHR (BML-SA210-0100, Enzo Life Sciences, Inc., Farmingdale, NY) and rabbit monoclonal anti-TSPO (ab109497, Abcam, Cambridge, UK). Anti-β-actin mouse monoclonal (sc-47778, Santa Cruz Biotechnology, Inc., Dallas, TX) was used as the loading control. The membranes were then labeled with either horseradish peroxidase (HRP) conjugated mouse anti-rabbit secondary (sc-2357, Santa Cruz Biotechnology, Inc., Dallas, TX) or HRP-conjugated mouse IgGκ light chain binding protein (sc-516102, Santa Cruz Biotechnology, Inc., Dallas, TX) according to host of primary antibody. Super Signal West Femto Maximum Sensitivity Substrate (Thermo Fisher Scientific, Waltham, MA). or Pierce™ ECL Western Blotting Substrate (Thermo Fisher Scientific, Waltham, MA) was used to visualize bands, Densitometry analysis was conducted using ImageJ (National Institutes of Health, Bethesda, MA). Bands were normalized to β-actin and compared to wild-type controls.

2.5 DNA Sequencing

DNA was isolated from cells using DNeasy Blood & Tissue Kit (Qiagen, Hilden, Germany). DNA was amplified using Q5 High-Fidelity DNA Polymerase (New England Biolabs, Ipswich, MA) as per manufacturer's protocol. The annealing temperatures for the PCR were 67°C for AHR and 71°C for TSPO.

PCR primers for *Ahr* 1.4 were:

Forward 5'-GAGTCTCCTCTGTCGCCCGC −3'

Reverse 5'-CCGTCACTCACGTTTTCT −3'

PCR primers for *Tspo* 1.1 were:

Forward 5'-GCCGTGGGCCTCACTCTGGTGC-3'

Reverse 5'-CTACCCCATGGCTGAATACAGTGTGC-3'

PCR primers for *Tspo* 2.2 were:

Forward 5'-GGAGCCTACTTTGTACGTGGC-3'

Reverse 5'-GATTCCAGGGGCAACAGAGCACAGC-3'

The PCR fragments were confirmed with 2% agarose gel electrophoresis and then sequenced using Sanger Sequencing 96 capillary electrophoretic ABI 3730xl platform

at the Michigan State University Research Technology Support Facility Genomics Core. Chromatograms were visualized using FinchTV Version 1.4.0 (Geospiza Inc., Seattle, WA).

2.6 Trypan Blue Cell growth curves

MLE-12 cells were plated at 40,000 cells per well in a 6-well dish. At each time point cells were removed from duplicate wells using trypsin solution (trypsin 0.25%, 1 mM EDTA, Hank's Balanced Salts). Cells were stained with trypan blue solution (0.4%, Sigma-Aldrich, St. Louis, MO) and counted using Bright-Line hemacytometer (Reichert, Buffalo, NY). Cell density was determined at approximately 23, 47, and 71 hours after plating. Four independent experiments were conducted.

2.7 MTT Cell Growth Curves

MLE-12 cells were plated at a density of 1,334 cells per well in a 96-well dish in technical triplicates. At 24, 48, and 72 hours after plating, old media was removed and replaced with cell culture media containing thiazolyl blue tetrazolium bromide (MTT) (0.5 mg/ml, Sigma-Aldrich, St. Louis, MO). Cells were incubated with MTT media for 1 hour in 37°C incubator. After incubation MTT media was removed and replaced with dimethyl sulfoxide (DMSO) (100%, Sigma-Aldrich, St. Louis, MO). Plates were wrapped in aluminum foil and agitated (25°C, 5 minutes). Absorbance was read at 570 nm using a FLUOstar Omega (BMG Labtech, Ortenberg, Germany). Wells without cells served as blanks and their average absorbance was subtracted from sample well absorbances.

2.8 RNA Collection and Sequencing

Wild-type, AHR−/−, and TSPO−/− MLE-12 cells were each treated with DMSO (0.003%) and ethanol (0.005%), 2,3,7,8-tetrachlorodibenzo-ρ-dioxin (TCDD, 10 nM) and ethanol (0.005%), 1-(2-chlorophenyl)-N-methyl-N-(1-methyl-propyl)-3-isoquinoline carboxamide (PK11195, 100 nM) and dimethyl sulfoxide (DMSO, 0.003%), or TCDD (10 nM) and PK11195 (100 nM) for 6 hours. Three biological replicates were conducted consisting of one technical replicate each. Cells were collected using TRIzol Reagent (Thermo Fisher Scientific, Waltham, MA) and RNA was isolated using protocol based on manufacturer's guide.

RNA concentration was determined using Qubit fluorometer (Thermo Fisher Scientific, Waltham, MA) and RNA quality was assessed by the MSU Genomics Core using an Agilent 2100 Bioanalyzer. All samples had to have a purity ≥ 6.8. RNA samples were sequenced, and the data analyzed by Novogene (Sacramento, CA) using Illumina PE150 technology. Genes that had an adjusted p-value of <0.05 were considered to be differentially expressed.

2.9 Quantitative Real-Time Polymerase Chain Reaction (qRT-PCR)

MLE-12 and Hepa1c1c7 cells were plated at density of 85,000 cells/well in 6 well dishes in technical triplicates. The cells were allowed to grow for approximately 48 hours before being collected using TRIzol Reagent (Thermo Fisher Scientific, Waltham, MA). RNA was isolated using protocol based on Thermo Fisher's guide. Complimentary DNA (cDNA) was generated using GoScript Reverse Transcriptase (Promega, Madison, WI) with a c1000 Touch Thermocycler (Bio-Rad Laboratories, Hercules, CA). Samples were analyzed using

SYBR Green PCR Master Mix (Applied Biosystems, Thermo Fisher Scientific, Waltham, MA) in QuantStudio 3 Real-Time PCR System (Applied Biosystems, Thermo Fisher Scientific, Waltham, MA). Gene expression was normalized using the geometric mean of 3 housekeeping genes, *Hprt*, *Actb,* and *18s*, and calculated using $\Delta\Delta C_T$ method. Primers used are described in Supplementary Table 1. Final comparisons were made as fold change to the wild-type control.

2.10 Statistics

Statistical analyses were performed using Astatsa or MiniTab Version 21.2 (MiniTab LCC, State College, PA), and Prism Version 9.5.1 (GraphPad Softwares, San Diego, CA). Differences across treatment groups were assessed with one-way analysis of variance (ANOVA) with a Tukey's pair-wise posthoc test with $p \leq 0.05$ considered significant.

3. Results

3.1 The AHR and TSPO share putative endogenous ligands

Though the AHR is most known for its role in regulating the body's response to exogenous chemicals, such as TCDD, some progress has been made in understanding the endogenous role of the receptor, specifically, with small molecules that can act as endogenous ligands. These molecules include cholesterol [24], heme and heme metabolites [25], as well as tryptophan derivatives, such as kynurenine and 6-formylindolo[3,2-b]carbazole (FICZ) [26,27]. Many of these same small molecules have also been reported to bind to TSPO, with the exception so far of tryptophan derivatives. To explore the possibility that kynurenine could also bind TSPO, fluorescence quenching binding experiments were performed. The results show that TSPO binds kynurenine in the high micromolar range and thus shares another putative endogenous ligand with AHR (Fig. 1). This further supports the possibility that some level of crosstalk exists in their signaling cascades.

3.2 Generation of AHR−/− and TSPO−/− MLE-12 cell lines

Given that the AHR and TSPO share many putative endogenous ligands, it was hypothesized that some degree of crosstalk existed between the two proteins. To test this hypothesis, knockout cell lines were created in mouse lung epithelial cells (MLE-12) for each protein via CRISPR/Cas9. Possible knockout candidates were isolated with puromycin selection and confirmed by western blot (Fig. 2C). The CRISPR target regions was sequenced using Sanger Sequencing to confirm that the reading frame had been disrupted in each mutant. The sequencing indicated that the AHR−/− cells had a 12 nucleotide deletion that began after the adenine in the protein start codon (Fig 2A). So, without the start signal present, no translation at all of the AHR protein would be expected to occur. The TSPO−/− cells had a single cytosine incorrectly inserted into the sequence (Fig 2A). This caused a frame shift mutation that caused an early termination so that only a 35 amino acid protein would be translated.

3.3 Characterization of AHR and TSPO knockout cell lines

To explore the possibility that the presence of either AHR or TSPO could affect the expression of the other, RNA-seq data was examined. *Tspo* mRNA was increased 1.30-

fold in AHR−/− cells compared to wild-type (padj = 9.58E-07) (Fig. 2B). This increased expression was not altered upon exposure to the AHR ligand, TCDD (10 nM, 6 hrs) in either wild-type or AHR−/− cells (data not shown). The level of *Tspo* mRNA decreased 1.88-fold in the TSPO−/− cells when compared to the AHR−/− cells (padj = 1.52E-29). It was also decreased 1.45-fold in TSPO−/− cells compared to wild-type cells (padj = 5.74E-10) (Fig. 2B). So, while the CRISPR process prevented whole TSPO protein synthesis, transcripts were still synthesized but at a lower level than non-transfected cells. Loss of TSPO did not change the expression of *Ahr* mRNA (Fig. 2B).

Since the level of mRNA does not always match actual protein concentration, the level of AHR and TSPO was analyzed through western blots (Fig. 2C). The level of TSPO increased about 2-fold in AHR−/− cells when compared to wild-type as calculated when using β-actin as a loading control ($p < 0.05$) (Fig. 2D). This significant increase agrees with the increase in mRNA described above. The level of AHR in TSPO −/− cells was not significantly different when compared to wild-type parental cells (Fig. 2D). On average the AHR protein amount in TSPO −/− cells was about 90% of the wild-type. This result also agrees with the RNA-seq data which did not show a difference at the transcript level. The mRNA and protein expression data indicates that AHR pathways exhibit signaling crosstalk with TSPO, but AHR expression is not influenced by TSPO abundance.

To determine if the absence of either AHR or TSPO caused a change in proliferation, cell viability was analyzed using trypan blue cell counting and MTT viability assays. For trypan blue measurements, cells were plated at density of 40,000 cells per well in 6-well dishes and then live cells were counted over a period of three days. The growth for all cell lines was essentially the same between initial plating and 71 hours with no significant differences (Fig. 3A). For the MTT assay cells were plated at a density of 1,334 cells per well in 96-well dishes and MTT assays were individually run for three days after plating. There was no significant difference in the conversion of MTT at any of the time points assayed (Fig. 3B).

3.4 Differential expression of nuclear genes in AHR−/− and TSPO−/− MLE-12 cell lines

The change in TSPO protein levels in the AHR−/− knockout cells suggests some level of crosstalk exists between the two proteins. To determine if this crosstalk has functional significance, RNA-seq was performed on RNA extracted from the three cell lines (i.e. WT, AHR−/−, and TSPO−/−) following treatment (6 hrs) of DMSO (0.003%) and ethanol (0.005%), TCDD (10 nM), PK11195 (100 nM), or TCDD + PK11195 (10 nM + 100 nM respectively). Globally, loss of AHR led to 1,125 differentially expressed genes (DEGs) when compared to WT cells (Fig. 4). In comparison, loss of TSPO led to 2,757 DEGs when compared to wild-type cells. Interestingly, there were 567 DEGs shared between these two groups. When AHR−/− cells were compared to TSPO−/− cells there were 3,041 DEGs. Of these, 729 were shared with the AHR−/− vs WT DEGs and 1,801 were shared with the TSPO−/− vs WT DEGs. Finally, a core set of 333 genes were different between all three comparisons. Included in this core set of genes was *Glutathione S-transferase kappa 1* (*Gstk1)* with expression that increased 3.88-fold in AHR−/− cells (padj=6.1E-12) compared to WT cells but decreased 171.29-fold in TSPO−/− cells when compared to WT cells (padj=1.9E-7). The *Gstk1* mRNA was decreased 664.43-fold (padj=3.12E-13) when

TSPO−/− cells were compared to AHR−/− cells. *Gstk1* is a phase II drug-metabolizing enzyme that can localize to mitochondria. Another of these genes, *ATP binding cassette subfamily A member 1 (Abca1),* is used to transport cholesterol (which can be a ligand for both proteins) across the plasma membrane. It was increased 1.96-fold in AHR−/− cells (padj=3.6E-15) when compared to WT cells but decreased 1.57-fold in TSPO−/− cells (padj=4.0E-4) when compared to WT cells. It was decreased 3.07-fold when TSPO−/− cells were compared to AHR−/− cells (padj=2.15E-33). These data support the hypothesis that loss of AHR or TSPO affects a set of genes with functions that could imply crosstalk exists between the two proteins.

3.5 Identifying AHR target genes that are susceptible to TSPO-mediated alterations in expression

The AHR regulates the expression of a core battery of genes. This group includes approximately 100 genes, including *Cytochrome P450 1A1* (*Cyp1a1*), *Cyp1a2*, *Cyp1b1*, *AHR repressor* (*Ahrr*), and *NAD(P)H quinone dehydrogenase 1* (*Nqo1*) [36,10,37, 38,39]. To determine if loss of TSPO could impact the expression of these genes, the RNA-seq data were analyzed in the three cells lines following exposure to TCDD (10 nM), PK11195 (100 nM) or TCDD + PK11195 (10 nM, 100 nM, respectively) for 6 hours. All five of these core AHR battery genes displayed increased expression in the wild type cells following exposure to TCDD; however, only *Cyp1b1* and *Nqo1* reached the level of significance (Table 1). Their expression was not altered by PK11195 alone. Three of the five genes showed an increased expression in wild-type cells following co-exposure to TCDD and PK11195, with *Cyp1b1* and *Nqo1* again being significant but not when compared to cells just treated with TCDD. As expected, none of the genes displayed a change in expression following any treatment in the AHR−/− cells (Table 1) providing another layer of validation for AHR knockout. Finally, in the TSPO−/− cells, three of the five genes were significantly upregulated when treated with TCDD or TCDD + PK11195 when compared to control treated cells within cell type (Table 1). Interestingly, the loss of TSPO led to a significant increase in *Cyp1a1* and *Cyp1b1* when treated with TCDD or TCDD + PK11195 when compared to wild-type cells within respective treatment group (Table 1). These results suggest that TSPO plays a role in modulating the level of induction of some key AHR target genes.

To determine the extent of TSPO's ability to modulate AHR-mediated transcription, global changes in expression were analyzed. To identify genes most susceptible to TSPO influence, TCDD-induced DEGs in wild type cells were analyzed for influence of loss of TSPO and/or co-treatment with PK11195. Treatment with TCDD led to 91 DEGs in wild-type cells, 132 DEGs in the TSPO−/− cells, and 1 DEG in the AHR−/− cells (Fig. 5A and data not shown). Treatment with PK11195 led to 0 DEGs in the wild-type cells, 1 DEG in the TSPO−/− cells, and 7 DEGs in the AHR−/− cells (Data not shown). Exposing the cells to both chemicals concurrently led to 120 DEGs in the wild-type cells, 114 DEGs in the TSPO− /− cells, and zero DEGs in the AHR−/− cells (Fig. 5A and data not shown). Of the 91 DEGs identified in TCDD-treated WT cells, 29 of them were no longer significantly changed in the TCDD-treated TSPO−/− when compared to control TSPO−/− cells (Fig. 5A). There were 70 additional genes that were significantly changed in the TCDD-treated TSPO−/− when compared to control TSPO−/− cells that were not in the TCDD-treated WT cells. These data

suggest that approximately a third of AHR target genes are susceptible to TSPO-mediated crosstalk. To limit the number of false positives, the original 91 DEGs were also compared to the DEGs following TCDD+PK11195 co-treatment in WT cells. Co-treatment led to 32 of the 91 genes no longer being significantly altered. When this set is compared to the 29 impacted by the loss of TSPO, there are 13 genes that overlap (Fig. 5A and B). These genes represent the core genes regulated by the AHR that are susceptible to TSPO-mediated activity. Included in this group was *Dhrs3,* which is a short-chain dehydrogenase/reductase, which can catalyze reactions involving steroids and retinoids. This is of note since these compounds are predicted to be ligands for TSPO. *Dhrs3* expression had been previously noted to be altered upon TCDD exposure, and its promoter region contains DREs [40].

3.6 Differential expression of mitochondrial genes in WT, AHR−/−, and TSPO−/− MLE-12 cells

Of the over 50,000 genes used in the RNA-seq dataset, 0.647% of the gene descriptions contained the word mitochondria. This percentage significantly increased to 1.33% for the list of DEGs when wild-type and AHR−/− cells were compared and to 1.92% for the list of DEGs between wild-type and TSPO−/− cells. This enrichment is not unexpected for a protein located in the outer mitochondrial membrane, such as TSPO, but it is for a nuclear transcription factor like AHR. The enrichment following loss of AHR supports the notion that the pool of AHR found within the mitochondria has functional significance [16].

The RNA-seq data was also used to analyze changes in genes located in the mitochondrial genome. Out of the 13 protein-encoding mitochondrial genes, seven were slightly but significantly upregulated in TSPO−/− cells and two were upregulated in AHR−/− cells (Fig. 6). *Nd3*, *Nd4l*, *Nd6*, *Co3*, and *Atp8* were the five genes that were not significantly altered in either of the knockout cell lines. NADH dehydrogenase 4 (*Nd4),* a subunit of respiratory complex I, was the one gene that was upregulated by the loss of both genes. Loss of TSPO had a larger impact on mitochondrial-encoded genes than loss of AHR, however both demonstrated the ability to alter the expression of genes that encode key subunits of the electron transport system.

3.7 Mitochondrial calcium transport alterations in AHR and TSPO knockout cell lines

Mitochondrial-involved calcium homeostasis and signaling is essential for all cells and is tightly controlled. One way that calcium can enter the mitochondrial matrix is via the mitochondrial calcium uniporter (MCU). The MCU is a multisubunit protein and loss of both AHR and TSPO altered the expression of MCU components. For example, loss of both proteins led to a drastic decrease of *Micu2* expression. *Micu2* expression was repressed 94.88-fold in the AHR−/− cells (padj=3.5E-05) and 94.08-fold in the TSPO −/− cells (padj=2.2E-05) compared to wild-type cells (Table 2). Loss of AHR caused an increase in expression of *Micu1* (1.17-fold, padj=1.7E-03) but this did not occur in TSPO−/− cells. Loss of TSPO caused a 1.3-fold (padj=3.0 E-02) increase in expression of *Micu3* but this did not occur in AHR−/− cells. *Mcu* was significantly decreased 1.28-fold (padj=4.2E-04) in TSPO−/− and non-significantly increased 1.16-fold (padj=6.0E-02) in AHR−/−. The gene for the SMDT1 (aka EMRE) subunit was not significantly altered in either of the mutant cell lines. It is unclear how much loss of AHR or TSPO affects total calcium within the

mitochondria, but it should be noted that there are mitochondrial exchangers that were not altered in either mutant cell line. *Letm1*, for example, encodes a Ca^{2+}/H^{+} antiporter located in the inner mitochondrial membrane that was not significantly changed in either AHR−/− or TSPO−/− mutants. Finally, treatment of WT, AHR−/− or TSPO−/− cells with TCDD, PK11195, or the combination of both did not alter the expression of any gene that encodes an MCU subunit.

3.8 Variation between cell types for RNA-seq differentially expressed genes

To determine if the changes in gene expression due to loss of AHR or TSPO was lung cell specific, CRISPR knockouts of AHR and TSPO were created in a mouse liver cell line (Hepa1c1c7, Fig. 7A–B). RNA was then collected from the MLE-12 and Hepa1c1c7 cells and analyzed using SYBR Green PCR protocol. Six DEGs from the MLE-12 RNA-seq data were compared: *Abca1*, *Gpr39*, *Gstk1*, *Micu2*, *Mt1*, and *Nfatc2* (Fig. 7C–H). None of the genes were significantly altered in the Hepa1c1c7 cells while *Abca1*, *Gpr39*, *Gstk1*, *Micu2*, and *Nfatc2* were significantly altered in the MLE-12 in at least one cell type. *Gpr39* had a similar trend between cell types with a decrease of 1.4-fold (p=0.4106) in the AHR−/− and 1.5-fold (p=0.3293) in the TSPO−/− Hepa1c1c7 cells and a significant decrease of 16.4-fold (p<0.0001) in the AHR−/− and 12.6-fold (p<0.0001) in the TSPO−/− MLE-12 cells (Fig. 7D). *Metallothionein 1* (*Mt1*) expression also followed a similar trend in the TSPO−/− cells, decreasing increased a nonsignificant 2.4-fold (p=0.2790) in Hepa1c1c7 AHR−/− but decreased a nonsignificant 2.0-fold (p=0.1137) in MLE-12 AHR−/− cells (Fig. 7G).

4. Discussion

The proper maintenance and growth of biological cells is a complex process requiring multiple proteins and various signaling pathways. The cell needs to be able to respond quickly to both endogenous and exogenous signals to alter activity for survival. The AHR and TSPO are two ligand-binding proteins that influence many pathways. The goal of this research was to explore the possibility that these two previously unlinked proteins might participate in crosstalk. This postulation was based on the discovery that there is considerable overlap between putative ligands for AHR and TSPO, raising the potential for these proteins to work together in response to those ligands or to respond to similar microenvironments.

Through analysis of gene expression, it was determined that there were categories of genes that were influenced by loss of the proteins and/or exposure to known ligands, that implied an overlap of functionality of the AHR and TSPO. For example, the level of TSPO mRNA and protein was increased in untreated AHR−/− cells compared to their wild-type counterparts. The increase in TSPO protein following the loss of AHR could be a mechanism to either compensate for a specific function of the AHR that needs to be maintained or to react to environment with more unbound AHR ligands. The exact mechanism that explains this link between AHR and TSPO levels is unknown; however, the AHR could modulate TSPO transcription directly or indirectly though activating another signaling pathway, such as mitochondria-to-nucleus stress signaling. Loss of TSPO, however, does not cause a similar increase in AHR mRNA or protein. This might provide

evidence against the AHR and TSPO working in the same physical pathway because the cell would normally be expected to try to make up for the loss of one step by altering expression of others. The protein analysis supports TSPO somehow being involved downstream of AHR activity.

The AHR is classically associated with enhancing drug metabolizing enzymes to protect the cell from foreign toxicants. The alteration in TSPO expression after AHR elimination suggests that TSPO also acts in those processes. To examine this, RNA expression of the two major AHR-linked Cytochrome P450s, *Cyp1a1* and *Cyp1b1*, was measured after TCDD (AHR ligand) treatment. It was found that the expression of both increased more in the TSPO−/− cells compared to the wild-type cells after 6 hours of TCDD exposure. This result indicates that either TSPO normally functions to dampen the expression of these P450 genes or its loss indirectly allows for increased AHR activity. Interestingly, this TSPO-dependent increase in *Cyp1a1* and *1b1* did not occur for all known AHR target genes suggesting that the signaling interaction between the AHR and TSPO might be context or cell-type specific.

CYP1B1 metabolizes many endogenous molecules including estradiol [41] and retinol [42]. These substrates for CYP1B1 might offer some clues as to why TSPO could dampen its AHR-mediated expression. Both estradiol and retinoic acid can modulate TSPO expression and retinoic acid can bind TSPO [43,44], directly linking their intracellular concentration to TSPO signaling. The ability of TSPO to modulate TCDD-induced *Cyp1a1* and *1b1* expression might also involve heme homeostasis. TSPO has been linked to regulating the concentration of other heme-dependent enzymes by acting as a source of heme for these molecules, such as NOX2 [45], so it could also provide this function for P450s. The fact that other cytochrome P450s were not influenced by loss of TSPO (i.e. *Cyp1a2*) does not support this model, meaning that the *Cyp1a1* and *1b1* expression increase could be specific. The level of *Cyp1A2*, however, is much lower in MLE-12s and might not act as the same heme sink as the other two isoforms.

The current model of AHR biology has the receptor only in the cytosol of the cell when unbound or in the nucleus when bound by a ligand. Tappenden et al. [17] and Hwang et al. [16] have suggested that a portion of the AHR can be located in mitochondria, allowing for the hypothesis that the receptor could influence mitochondrial activity. The RNA-sequencing data also show that loss of either TSPO or AHR impacted a significantly larger number of mitochondrial-associated genes than would be expected just by chance. The AHR−/− cells having an enrichment of mitochondrial DEGs similar to a known mitochondrial protein strengthens the possibility of mitoAHR. Some of these genes were nuclear-encoded genes but some were mitochondrial-encoded. Of the mitochondrial-encoded genes altered by AHR and TSPO loss, all of them exhibited increased expression. The reason for this increase is unknown; however, the AHR can induce mitochondrial stress and decrease the organelle's oxidative phosphorylation efficiency [17]. Directly linking AHR to maintenance of the expression of genes necessary for mitochondrial function, such as *Nd1* and *Nd4*, might be evidence of a way for the cell to maintain proper cellular energetics following modulation of the receptor's activity.

The link between mitochondrial function and calcium signaling provides clues to the possible role of crosstalk between TSPO and AHR for cellular homeostasis. There are multiple calcium channels in mitochondria and the mitochondrial calcium uniporter (MCU) is a major entrance for calcium into the mitochondrial matrix from the intermembrane space. The MCU is a 480 kDa transmembrane protein complex that varies in protein composition between species, but the core MCU protein is highly conserved [46,47]. The other proteins comprising the murine MCU are the mitochondrial calcium uptake 1 (MICU1) [48], the mitochondrial calcium uptake 2 (MICU2) [49], and the single-pass membrane protein with aspartate rich tail 1 (SMDT1, aka EMRE) [47]. The MCU and SMDT1 proteins make up the transmembrane portion of complex and MICU1 and MICU2 are located on the intermembrane space side to control calcium entry [50]. It is currently proposed that at low intermembrane calcium levels, the MICU proteins act to prevent the entry of calcium ions into the matrix [51]. At high intermembrane calcium levels, this inhibition is removed and allows for the increase of the matrix calcium level. The data showed that loss of both AHR and TSPO caused the expression of *Micu2* to decrease to an undetectable level within untreated MLE-12 cells. The predicted location of AHR and TSPO could provide some clues as to why they influence expression of components in the MCU. Hwang et al. [16] showed that a portion of the cellular pool of AHR is located within the intermembrane space, so it is possible that the receptor could physically interact with the MICU2 protein projecting into that region. TSPO is known to interact with VDAC in the outer membrane of mitochondria [52], which functions to allow transport of molecules into the intermembrane space including calcium. These calcium ions could then be funneled into the mitochondrial matrix through the MCU. Gatliff et al. [32] found that loss of TSPO caused an elevation of calcium uptake into mitochondria after ATP stimulation. This would match the proposal that TSPO limits calcium uptake through VDAC and supports the observation of the decrease in *Micu2* expression in TSPO−/− cells. The cells could be trying to remove the inhibition of calcium flow into the MCU as a reaction to the higher concentration of calcium in the intermembrane space. The ability of AHR and TSPO to modulate the gene expression of components of the MCU is a possible mechanism for the two proteins to modulate mitochondrial function by regulating the entry of calcium into the matrix.

Most functions of the AHR have been attributed to nuclear DNA binding but a growing number of AHR-dependent outcomes have suggested that this might not be the only utility of the receptor. Independent of DNA binding, agonists of the receptor can still elicit effects including altering cholesterol synthesis proteins [53] and cell cycle progress [54]. The AHR would also not be the first transcription factor receptor to be proposed to be located in mitochondria as the estrogen receptor [18,19], glucocorticoid receptor [20,21], and thyroid receptor [22,23] have all been detected there. There is even evidence that certain hormones have the ability to influence mitochondrial RNA synthesis including thyroid hormone [55] and glucocorticoids [56]. The AHR could similarly act to modulate mitochondrial activity.

In an attempt to determine the level of cell-type specificity of these results, two additional CRISPR cell lines were created for AHR and TSPO knockouts in a mouse liver line (Hepa1c1c7). The RNA gene expression experiments comparing the MLE-12 and Hepa1c1c7 indicated that the functions of AHR and TSPO tend to vary between cell types. While cell lines have been immortalized, they still retain characteristics of their

tissue of origin. It is possible that AHR and TSPO have different functions in lung cells versus liver cells due to the interaction with other cell-type specific protein expression. For example, ABCA1 is used to transport cholesterol out of the cell across the plasma membrane and cholesterol regulation is most likely very different be very different in the two tissues [57]. For example, the liver is primarily a cholesterol producing organ, while this is not the case for the lung and, therefore, the different expression patterns observed in the MLE12 vs. Hepa1c1c7 is understandable. *Gpr39* was the only gene analyzed that showed similar expression pattern in both cell types. G-Protein Coupled Receptor 39 (GPR39) is classified as an orphan receptor, but zinc has been proposed to be an endogenous ligand [58]. Currently no direct link has been established between AHR or TSPO and GPR39. GRP39, when overexpressed, has been found to prevent lipid accumulation and reduce mitochondrial stress in a liver cell model of non-alcoholic fatty liver disease (NAFLD) [59]. Taken together, these finding might suggest that GPR39 is regulated in at AHR- and/or TSPO-dependent manner to maintain mitochondrial homeostasis. More studies across cell types will be needed to understand the complex relationship between AHR and TSPO.

5. Conclusions

This report has collected evidence to show that the AHR and TSPO respond to similar ligands and are involved in related cellular processes in MLE-12 cells. The AHR was shown to alter TSPO concentration in MLE-12s at both the mRNA and protein level. Treatment with the AHR ligand, TCDD, demonstrated that TSPO could alter expression of AHR battery genes. Both genes were found to alter mitochondrial genes that are involved in oxidative phosphorylation and calcium transport. Further study is required to fully understand the role this crosstalk plays in cellular function and, specifically, mitochondrial homeostasis.

Supplementary Material

Refer to Web version on PubMed Central for supplementary material.

Acknowledgments

The authors would like to thank the Michigan State University Research Technology Support Facility Genomics Core for assistance in sequencing CRISPR knockout cell lines and assessing quality of RNA used for RNAseq.

Funding:

This work was supported by the National Institutes of Health [grant numbers 2P42ES004911];

Abbreviations

ABCA1	ATP binding cassette subfamily A member 1
AHR	aryl hydrocarbon receptor
AIP	AHR interacting protein
AHRR	AHR repressor

ARNT	aryl hydrocarbon nuclear translocator
CRISPR	Clustered regularly interspaced short palindromic repeats
Cas9	CRISPR associated protein 9
CYP1A1	Cytochrome P450 Family 1 Subfamily A Member 1
CYP1B1	Cytochrome P450 Family 1 Subfamily B Member 1
DHRS3	Dehydrogenase/Reductase 3
DREs	dioxin response elements
FICZ	6-formylindolo[3,2-b]carbazole
GPR39	G-protein coupled receptor 39
GSTK1	Glutathione S-transferase kappa 1
MCU	mitochondrial calcium uniporter
MICU	mitochondrial calcium uptake
mitoAHR	mitochondrial localized AHR
MLE-12	murine lung epithelial cell line 12
MT1	metallothionein 1
NFATC2	nuclear factor of activated t cells 2
PBR	peripheral-type benzodiazepine receptor
NQO1	NAD(P)H quinone dehydrogenase 1
PK11195	1-(2-chlorophenyl)-*N*-methyl-*N*-(1-methylpropyl)-3-isoquinolinecarboxamide
RsTSPO	Rhodobacter spheroids TSPO
SMDT1	single-pass membrane protein with aspartate rich tail 1
TCDD	2,3,7,8-tetrachlorodibenzo-ρ-dioxin
TSPO	translocator protein
VDAC	voltage-dependent anion channel

References

[1]. Poland A, Glover E, and Kende AS, 1976. Stereospecific, high affinity binding of 2,3,7,8-tetrachlorodibenzo-p-dioxin by hepatic cytosol. Evidence that the binding species is receptor for induction of aryl hydrocarbon hydroxylase. J. Biol. Chem 251 (16), 4936–4946. [PubMed: 956169]

[2]. Burbach KM, Poland A, & Bradfield CA, 1992. Cloning of the Ah-receptor cDNA reveals a distinctive ligand-activated transcription factor. Proc. Natl. Acad. Sci. USA 89 (17), 8185–8189. 10.1073/pnas.89.17.8185. [PubMed: 1325649]

[3]. Carver LA, LaPres JJ, Jain S, Dunham EE, & Bradfield CA, 1998. Characterization of the Ah receptor-associated protein, ARA9. J. Biol. Chem 273 (50), 33580–33587. 10.1074/jbc.273.50.33580. [PubMed: 9837941]

[4]. Meyer BK, Pray-Grant MG, Vanden Heuvel JP, & Perdew GH, 1998. Hepatitis B virus X-associated protein 2 is a subunit of the unliganded aryl hydrocarbon receptor core complex and exhibits transcriptional enhancer activity. Mol. Cell Biol 18 (2), 978–988. 10.1128/MCB.18.2.978. [PubMed: 9447995]

[5]. Meyer BK, & Perdew GH, 1999. Characterization of the AhR-hsp90-XAP2 core complex and the role of the immunophilin-related protein XAP2 in AhR stabilization. Biochemistry 38 (28), 8907–8917. 10.1021/bi982223w. [PubMed: 10413464]

[6]. Perdew GH, 1988. Association of the Ah receptor with the 90-kDa heat shock protein. J. Biol. Chem 263 (27), 13802–13805. [PubMed: 2843537]

[7]. Probst MR, Reisz-Porszasz S, Agbunag RV, Ong MS, & Hankinson O, 1993. Role of the aryl hydrocarbon receptor nuclear translocator protein in aryl hydrocarbon (dioxin) receptor action. Mol Pharmacol. 44(3), 511–518. [PubMed: 8396713]

[8]. Denison MS, Fisher JM, and Whitlock JP, 1988. The DNA recognition site for the dioxin-Ah receptor complex. Nucleotide sequence and functional analysis. J. Biol. Chem 263 (33), 17221–17224. [PubMed: 2846558]

[9]. Nukaya M, & Bradfield CA, 2009. Conserved genomic structure of the Cyp1a1 and Cyp1a2 loci and their dioxin responsive elements cluster. Biochem. Pharmacol 77(4):654–659. doi:10.1016/j.bcp.2008.10.026. [PubMed: 19026991]

[10]. Sutter TR, Tang YM, Hayes CL, Wo YY, Jabs EW, Li X, Yin H, Cody CW, & Greenlee WF, 1994. Complete cDNA sequence of a human dioxin-inducible mRNA identifies a new gene subfamily of cytochrome P450 that maps to chromosome 2. J. Biol. Chem 269 (18), 13092–13099. [PubMed: 8175734]

[11]. Zhou Y,Tung HY, Tsai YM, Hsu SC, Chang HW, Kawasaki H, Tseng HC, Plunkett B, Gao P, Hung CH, Vonakis BM, & Huang SK, 2013. Aryl hydrocarbon receptor controls murine mast cell homeostasis. Blood 121 (16), 3195–3204. 10.1182/blood-2012-08-453597. [PubMed: 23462117]

[12]. Brinchmann BC, Le Ferrec E, Bisson WH, Podechard N, Huitfeldt HS, Gallais I, Sergent O, Holme JA, Lagadic-Gossmann D, & Øvrevik J, 2018. Evidence of selective activation of aryl hydrocarbon receptor nongenomic calcium signaling by pyrene. Biochem. Pharmacol 158, 1–12. 10.1016/j.bcp.2018.09.023. [PubMed: 30248327]

[13]. Sánchez-Martín FJ, Fernández-Salguero PM, & Merino JM, 2011. Aryl hydrocarbon receptor-dependent induction of apoptosis by 2,3,7,8-tetrachlorodibenzo-p-dioxin in cerebellar granule cells from mouse. J. Neurochem 118 (1), 153–162. 10.1111/j.1471-4159.2011.07291.x. [PubMed: 21534955]

[14]. Jang HS, Pearce M, O'Donnell EF, Nguyen BD, Truong L, Mueller MJ, Bisson WH, Kerkvliet NI, Tanguay RL, & Kolluri SK, 2017. Identification of a Raloxifene Analog That Promotes AhR-Mediated Apoptosis in Cancer Cells. Biology 6 (4). 10.3390/biology6040041.

[15]. Park WH, Jun DW, Kim JT, Jeong JH, Park H, Chang YS, Park KS, Lee HK, & Pak YK, 2013. Novel cell-based assay reveals associations of circulating serum AhR-ligands with metabolic syndrome and mitochondrial dysfunction. Biofactors. 39 (4), 494–504. 10.1002/biof.1092. [PubMed: 23361953]

[16]. Hwang HJ, Dornbos P, Steidemann M, Dunivin TK, Rizzo M, & LaPres JJ 2016. Mitochondrial-targeted aryl hydrocarbon receptor and the impact of 2,3,7,8-tetrachlorodibenzo-p-dioxin on cellular respiration and the mitochondrial proteome. Toxicol. Appl. Pharmacol 304, 121–132. 10.1016/j.taap.2016.04.005. [PubMed: 27105554]

[17]. Tappenden DM, Lynn SG, Crawford RB, Lee K, Vengellur A, Kaminski NE, Thomas RS, & LaPres JJ, 2011. The aryl hydrocarbon receptor interacts with ATP5α1, a subunit of the ATP synthase complex, and modulates mitochondrial function. Toxicol. Appl. Pharmacol 254 (3), 299–310. 10.1016/j.taap.2011.05.004. [PubMed: 21616089]

[18]. Cammarata PR, Chu S, Moor A, Wang Z, Yang SH, & Simpkins JW, 2004. Subcellular distribution of native estrogen receptor alpha and beta subtypes in cultured human lens epithelial cells. Exp. Eye Res 78 (4), 861–871. 10.1016/j.exer.2003.09.027. [PubMed: 15037120]

[19]. Yang SH, Liu R, Perez EJ, Wen Y, Stevens SM, Valencia T, Brun-Zinkernagel AM, Prokai L, Will Y, Dykens J, Koulen P, & Simpkins JW, 2004. Mitochondrial localization of estrogen receptor beta. Proc. Natl. Acad. Sci. USA 101 (12), 4130–4135. 10.1073/pnas.0306948101. [PubMed: 15024130]

[20]. Scheller K, Sekeris CE, Krohne G, Hock R, Hansen IA, & Scheer U, 2000. Localization of glucocorticoid hormone receptors in mitochondria of human cells. Eur. J. Cell Biol 79 (5), 299–307. 10.1078/S0171-9335(04)70033-3. [PubMed: 10887960]

[21]. Psarra AM, Solakidi S, Trougakos IP, Margaritis LH, Spyrou G, & Sekeris CE, 2005. Glucocorticoid receptor isoforms in human hepatocarcinoma HepG2 and SaOS-2 osteosarcoma cells: presence of glucocorticoid receptor alpha in mitochondria and of glucocorticoid receptor beta in nucleoli. Int. J. Biochem. Cell Biol 37 (12), 2544–2558. 10.1016/j.biocel.2005.06.015. [PubMed: 16076561]

[22]. Hashizume K, & Ichikawa K, 1982. Localization of 3,5,3'-L-triiodothyronine receptor in rat kidney mitochondrial membranes. Biochem. Biophys. Res. Commun 106 (3), 920–926. 10.1016/0006-291x(82)91798-3. [PubMed: 6288037]

[23]. Morrish F, Buroker NE, Ge M, Ning XH, Lopez-Guisa J, Hockenbery D, & Portman MA, 2006. Thyroid hormone receptor isoforms localize to cardiac mitochondrial matrix with potential for binding to receptor elements on mtDNA. Mitochondrion 6 (3), 143–148. 10.1016/j.mito.2006.04.002. [PubMed: 16730242]

[24]. Savouret JF, Antenos M, Quesne M, Xu J, Milgrom E, & Casper RF, 2001. 7-ketocholesterol is an endogenous modulator for the arylhydrocarbon receptor. J. Biol. Chem 276 (5), 3054–3059. 10.1074/jbc.M005988200. [PubMed: 11042205]

[25]. Phelan D, Winter GM, Rogers WJ, Lam JC, & Denison MS, 1998. Activation of the Ah receptor signal transduction pathway by bilirubin and biliverdin. Arch. Biochem. Biophys 357 (1), 155–163. 10.1006/abbi.1998.0814. [PubMed: 9721195]

[26]. Mezrich JD, Fechner JH, Zhang X, Johnson BP, Burlingham WJ, & Bradfield CA, 2010. An interaction between kynurenine and the aryl hydrocarbon receptor can generate regulatory T cells. J. Immunol 185 (6), 3190–3198. 10.4049/jimmunol.0903670. [PubMed: 20720200]

[27]. Seok SH, Ma ZX, Feltenberger JB, Chen H, Scarlett C, Lin Z, Satyshur KA, Cortopassi M, Jefcoate CR, Ge Y, Tang W, Bradfield CA, & Xing Y, 2018. Trace derivatives of kynurenine potently activate the aryl hydrocarbon receptor (AHR). J. Biol. Chem 293 (6), 1994–2005. 10.1074/jbc.RA117.000631. [PubMed: 29279331]

[28]. Braestrup C, & Squires RF, 1977. Specific benzodiazepine receptors in rat brain characterized by high-affinity (3H) diazepam binding. Proc. Natl. Acad. Sci. USA 74 (9), 3805–3809. 10.1073/pnas.74.9.3805. [PubMed: 20632]

[29]. Li F, Xia Y, Meiler J, & Ferguson-Miller S, 2013. Characterization and modeling of the oligomeric state and ligand binding behavior of purified translocator protein 18 kDa from Rhodobacter sphaeroides. Biochemistry 52 (34), 5884–5899. 10.1021/bi400431t. [PubMed: 23952237]

[30]. Taketani S, Kohno H, Furukawa T, & Tokunaga R, 1995. Involvement of peripheral-type benzodiazepine receptors in the intracellular transport of heme and porphyrins. J. Biochem 117 (4), 875–880. 10.1093/oxfordjournals.jbchem.a124790. [PubMed: 7592553]

[31]. Azarashvili T, Krestinina O, Baburina Y, Odinokova I, Grachev D, Papadopoulos V, Akatov V, Lemasters JJ, & Reiser G, 2015. Combined effect of G3139 and TSPO ligands on Ca (2+)-induced permeability transition in rat brain mitochondria. Arch. Biochem. Biophys 587, 70–77. 10.1016/j.abb.2015.10.012. [PubMed: 26498031]

[32]. Gatliff J, East DA, Singh A, Alvarez MS, Frison M, Matic I, Ferraina C, Sampson N, Turkheimer F, & Campanella M, 2017. A role for TSPO in mitochondrial Ca. Cell Death Dis. 8 (6), e2896. 10.1038/cddis.2017.186. [PubMed: 28640253]

[33]. Zeno S, Zaaroor M, Leschiner S, Veenman L, & Gavish M, 2009. CoCl(2) induces apoptosis via the 18 kDa translocator protein in U118MG human glioblastoma cells. Biochemistry 48 (21), 4652–4661. 10.1021/bi900064t. [PubMed: 19358520]

[34]. Cui Y, Liang Y, Ip MSM, & Mak JCW, 2021. Cigarette smoke induces apoptosis via 18 kDa translocator protein in human bronchial epithelial cells. Life Sci. 265, 118862. 10.1016/j.lfs.2020.118862. [PubMed: 33301812]

[35]. Ran FA, Hsu PD, Wright J, Agarwala V, Scott DA, & Zhang F, 2013. Genome engineering using the CRISPR-Cas9 system. Nat. Protoc 8 (11), 2281–2308. 10.1038/nprot.2013.143. [PubMed: 24157548]

[36]. Pendurthi UR, Okino ST, Tukey RH, 1993. Accumulation of the nuclear dioxin (Ah) receptor and transcriptional activation of the mouse Cyp1a-1 and Cyp1a-2 genes. Arch Biochem Biophys. 306(1), 65–69. 10.1006/abbi.1993.1481. [PubMed: 8215422]

[37]. Xu L, Li AP, Kaminski DL, & Ruh MF, 2000. 2,3,7,8 Tetrachlorodibenzo-p-dioxin induction of cytochrome P4501A in cultured rat and human hepatocytes. Chem. Biol. Interact 124 (3), 173–189. 10.1016/s0009-2797(99)00149-0. [PubMed: 10728777]

[38]. Mimura J, Ema M, Sogawa K, & Fujii-Kuriyama Y, 1999. Identification of a novel mechanism of regulation of Ah (dioxin) receptor function. Genes Dev. 13 (1), 20–25. 10.1101/gad.13.1.20. [PubMed: 9887096]

[39]. Favreau LV, & Pickett CB, 1991. Transcriptional regulation of the rat NAD(P)H:quinone reductase gene. Identification of regulatory elements controlling basal level expression and inducible expression by planar aromatic compounds and phenolic antioxidants. J. Biol. Chem 266 (7), 4556–4561. [PubMed: 1900296]

[40]. Boverhof DR, Burgoon LD, Tashiro C, Chittim B, Harkema JR, Jump DB, & Zacharewski TR, 2005. Temporal and dose-dependent hepatic gene expression patterns in mice provide new insights into TCDD-Mediated hepatotoxicity. Toxicol. Sci 85 (2), 1048–1063. 10.1093/toxsci/kfi162. [PubMed: 15800033]

[41]. Hayes CL, Spink DC, Spink BC, Cao JQ, Walker NJ, Sutter TR,1996. 17 beta-estradiol hydroxylation catalyzed by human cytochrome P450 1B1. Proc. Natl. Acad. Sci. USA 93(18),9776–9781. 10.1073/pnas.93.18.9776. [PubMed: 8790407]

[42]. Chambers D, Wilson L, Maden M, & Lumsden A, 2007. RALDH-independent generation of retinoic acid during vertebrate embryogenesis by CYP1B1. Development 134(7):1369–1383. 10.1242/dev.02815. [PubMed: 17329364]

[43]. Chen C, Kuo J, Wong A, & Micevych P, 2014. Estradiol modulates translocator protein (TSPO) and steroid acute regulatory protein (StAR) via protein kinase A (PKA) signaling in hypothalamic astrocytes. Endocrinology 155 (8), 2976–2985. 10.1210/en.2013-1844. [PubMed: 24877623]

[44]. González-Blanco L, Bermejo-Millo JC, Oliveira G, Potes Y, Antuña E, Menéndez-Valle I, Vega-Naredo I, Coto-Montes A, & Caballero B, 2021. Neurogenic Potential of the 18-kDa Mitochondrial Translocator Protein (TSPO) in Pluripotent P19 Stem Cells. Cells 10 (10). 10.3390/cells10102784.

[45]. Guilarte TR, Loth MK, & Guariglia SR, 2016. TSPO Finds NOX2 in Microglia for Redox Homeostasis. Trends Pharmacol. Sci 37 (5), 334–343. 10.1016/j.tips.2016.02.008. [PubMed: 27113160]

[46]. Baughman JM, Perocchi F, Girgis HS, Plovanich M, Belcher-Timme CA, Sancak Y, Bao XR, Strittmatter L, Goldberger O, Bogorad RL, Koteliansky V, & Mootha VK, 2011. Integrative genomics identifies MCU as an essential component of the mitochondrial calcium uniporter. Nature 476(7360), 341–345. 10.1038/nature10234. [PubMed: 21685886]

[47]. Sancak Y, Markhard AL, Kitami T, Kovács-Bogdán E, Kamer KJ, Udeshi ND, Carr SA, Chaudhuri D, Clapham DE, Li AA, Calvo SE, Goldberger O, Mootha VK, 2013. EMRE is an essential component of the mitochondrial calcium uniporter complex. Science 342(6164), 1379–1382. 10.1126/science.1242993. [PubMed: 24231807]

[48]. Perocchi F, Gohil VM, Girgis HS, Bao XR, McCombs JE, Palmer AE, & Mootha VK, 2010. MICU1 encodes a mitochondrial EF hand protein required for Ca (2+) uptake. Nature 467(7313):291–296. 10.1038/nature09358. [PubMed: 20693986]

[49]. Plovanich M, Bogorad RL, Sancak Y, Kamer KJ, Strittmatter L, Li AA, Girgis HS, Kuchimanchi S, De Groot J, Speciner L, Taneja N, O'Shea J, Koteliansky V, Mootha VK, 2013. MICU2, a paralog of MICU1, resides within the mitochondrial uniporter complex to regulate calcium handling. PLoS One. 8(2), e55785. 10.1371/journal.pone.0055785. [PubMed: 23409044]

[50]. Csordás G, Golenár T, Seifert EL, Kamer KJ, Sancak Y, Perocchi F, Moffat C, Weaver D, Perez S, Bogorad R, Koteliansky V, Adijanto J, Mootha VK & Hajnóczky G, 2013. MICU1 controls both the threshold and cooperative activation of the mitochondrial Ca2+ uniporter. Cell Metab. 17(6), 976–987. 10.1016/j.cmet.2013.04.020. [PubMed: 23747253]

[51]. Payne R, Hoff H, Roskowski A, Foskett JK, 2017. MICU2 Restricts Spatial Crosstalk between InsP3R and MCU channels by regulating threshold and gain of MICU1-mediated inhibition and activation of MCU. Cell Rep. 21(11), 3141–3154. 10.1016/j.celrep.2017.11.064. [PubMed: 29241542]

[52]. McEnery MW, Snowman AM, Trifiletti RR, & Snyder SH, 1992. Isolation of the mitochondrial benzodiazepine receptor: association with the voltage-dependent anion channel and the adenine nucleotide carrier. Proc. Natl. Acad. Sci. USA 89(8), 3170–3174. 10.1073/pnas.89.8.3170. [PubMed: 1373486]

[53]. Tanos R, Patel RD, Murray IA, Smith PB, Patterson AD, Perdew GH,2012. Aryl hydrocarbon receptor regulates the cholesterol biosynthetic pathway in a dioxin response element-independent manner. Hepatology 55(6):1994–2004. 10.1002/hep.25571. [PubMed: 22234961]

[54]. Köhle C, Gschaidmeier H, Lauth D, Topell S, Zitzer H, Bock KW, 1999. 2,3,7,8-Tetrachlorodibenzo-p-dioxin (TCDD)-mediated membrane translocation of c-Src protein kinase in liver WB-F344 cells. Arch Toxicol. 73(3), 152–158. 10.1007/s002040050600. [PubMed: 10401681]

[55]. Barsano CP, Degroot LJ, & Getz GS, 1977. The effect of thyroid hormone on in vitro rat liver mitochondrial RNA synthesis. Endocrinology 100(1), 52–60. 10.1210/endo-100-1-52. [PubMed: 830546]

[56]. Van Itallie CM,1992. Dexamethasone treatment increases mitochondrial RNA synthesis in a rat hepatoma cell line. Endocrinology 130(2), 567–576. 10.1210/endo.130.2.1370790. [PubMed: 1370790]

[57]. Chen L, Zhao Z, Zeng P, Zhou Y, Yin W, 2022. Molecular mechanisms for ABCA1-mediated cholesterol efflux. Cell Cycle 21(11), 1121–1139.10.1080/15384101.2022.2042777 [PubMed: 35192423]

[58]. Holst B, Egerod KL, Schild E, Vickers SP, Cheetham S, Gerlach L, Storjohann L, Stidsen CE, Jones R, Beck-Sickinger AG, Schwartz TW, 2007. GPR39 signaling is stimulated by zinc ions but not by obestatin. Endocrinology 148(1), 13–20. 10.1210/en.2006-0933 [PubMed: 16959833]

[59]. Chen Q, Lou Y, 2023. G protein-coupled receptor 39 alleviates mitochondrial dysfunction and hepatocyte lipid accumulation via SIRT1/Nrf2 signaling. J Bioenerg Biomembr. 55(1), 3–42. 10.1007/s10863-022-09953-4

Highlights:

- The aryl hydrocarbon receptor and translocator protein exhibit crosstalk
- This crosstalk is exhibited through gene expression and AHR and TSPO protein
- Transcriptionally, the crosstalk disproportionally affects mitochondrial genes.
- The two proteins play a major role in basal regulation of MICU2.

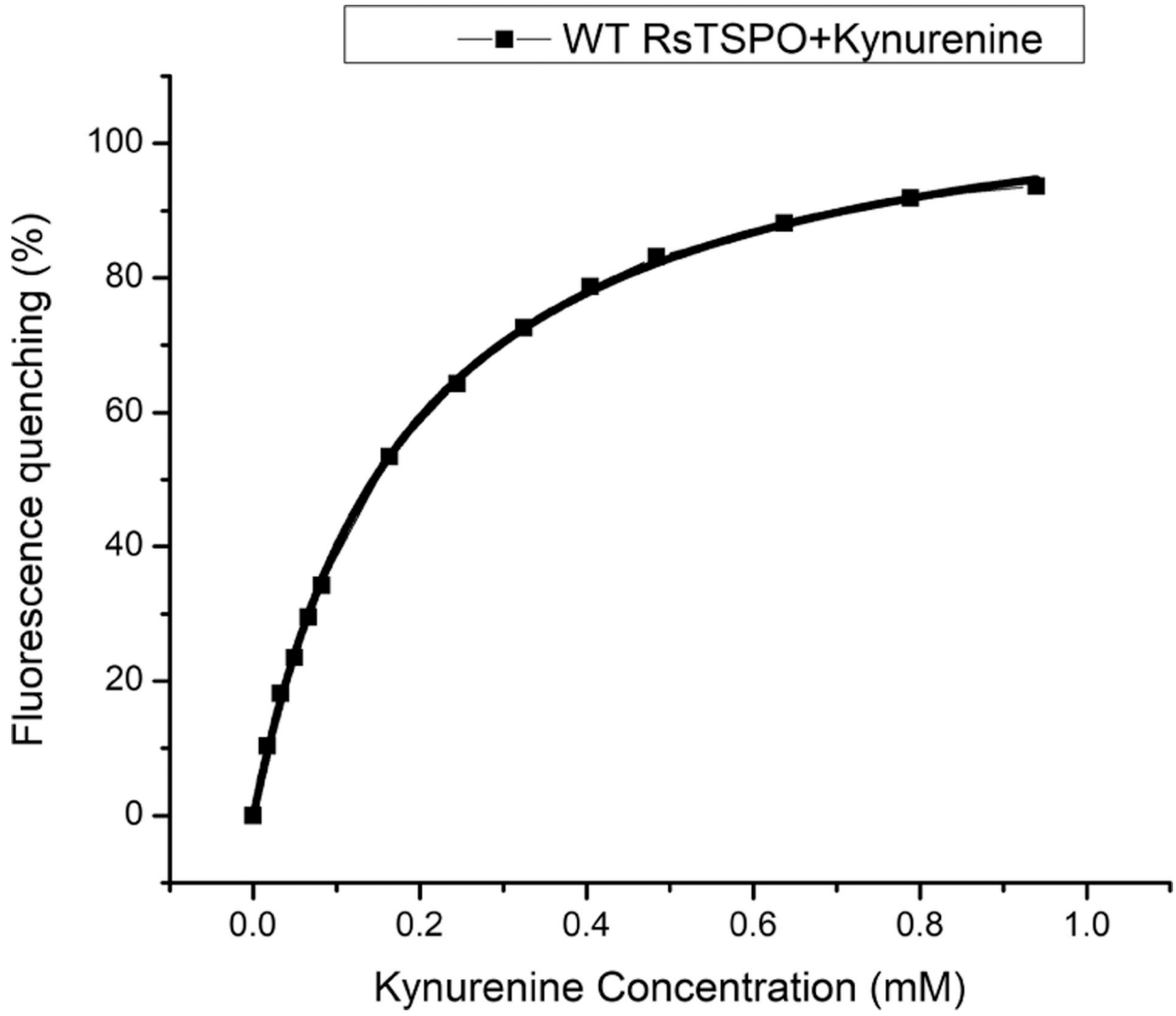

Fig. 1. Binding curve of Kynurenine with WT RsTSPO.

Kynurenine binding affinity to TSPO was determined via tryptophan fluorescent quenching as described in Material and Methods. The dissociation constant K_d=0.172±0.011 (mM) is calculated from three repeated experiments

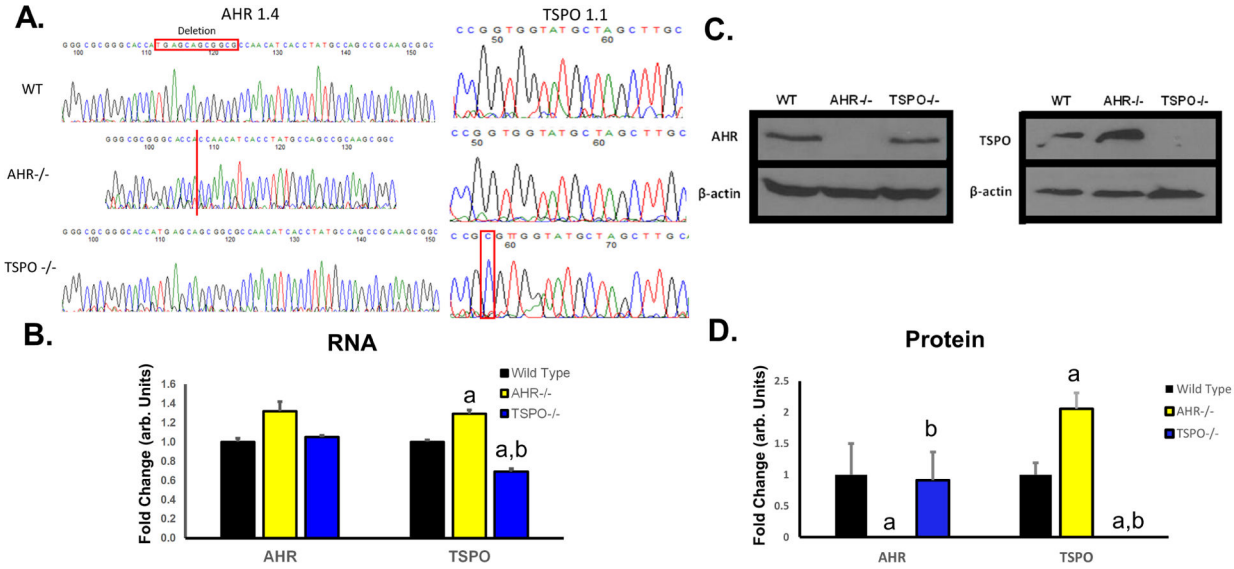

Fig. 2. Genomic, mRNA, and protein expression of AHR and TSPO in wild-type (WT), AHR−/−, and TSPO−/− MLE-12 cells.

Genomic DNA was extracted from MLE-12 cells using Qiagen DNeasy Blood & Tissue Kit, respective CRISPR region PCR amplified, and analyzed using Sanger Sequencing. Red boxes indicate region of change in knockout mutant (**A**). RNAseq data were analyzed for the expression AHR and TSPO in wild type (WT), AHR−/−, and TSPO−/− cells and shown relative to WT cells. a=significance from WT padj<0.05. b=significance from AHR−/− padj<0.05. n=3 (**B**). MLE-12s were grown to exponential growth phase and then collected in RIPA buffer. Whole cell protein (200 μg for AHR and 150 μg for TSPO) was separated by SDS-PAGE and protein was transferred to nitrocellulose and probed for AHR, TSPO, or β-actin (loading control) (**C**). Protein levels were normalized with loading control and then compared to WT levels. a=significance from WT padj<0.05. b=significance from AHR−/− padj<0.05. n≥3 (**D**).

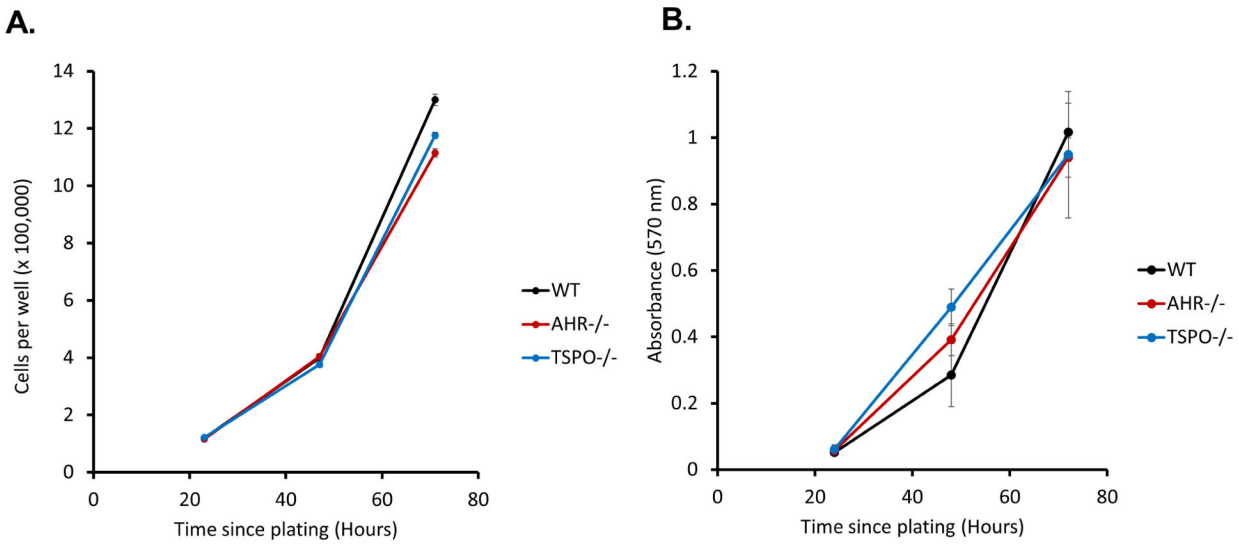

Fig. 3. Growth curves of wild-type (WT), AHR−/−, and TSPO−/− MLE-12 cells.

Cells were plated at an initial density of 40,000 cells per well in 6-well dishes. Two technical replicates were examined at each time point. Cells were removed from the well using 0.25% trypsin-1 mM EDTA, stained with 0.4% trypan blue, and counted using a hemacytometer. A total of four independent experiments were conducted. Error bars represent standard error **(A)** Cell were plated at an initial density of 1,334 cells per well in 96-well dish in technical triplicates. At each time point, media was removed and replaced with 0.5 mg/ml MTT media. After 1 hour incubation, MTT media was removed and replaced with 100% DMSO. Absorbance was read at 570 nm. A total of three independent experiments were conducted. Error bars represent standard error (**B**).

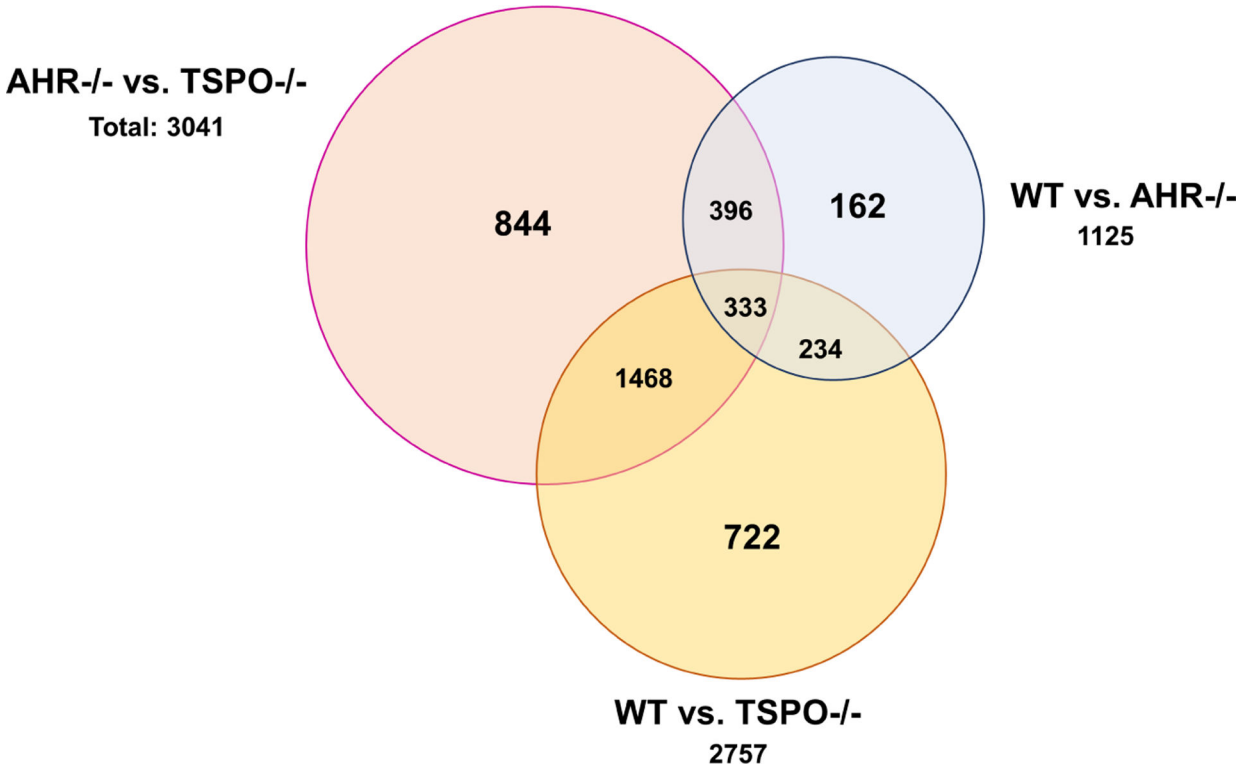

Fig. 4. Differentially expressed genes between untreated wild-type (WT), AHR−/−, and TSPO−/− MLE-12 cells.

RNA was isolated from cells using TRIzol protocol and sequenced by Novogene. Genes were considered significantly changed if padj value was <0.05. n=3

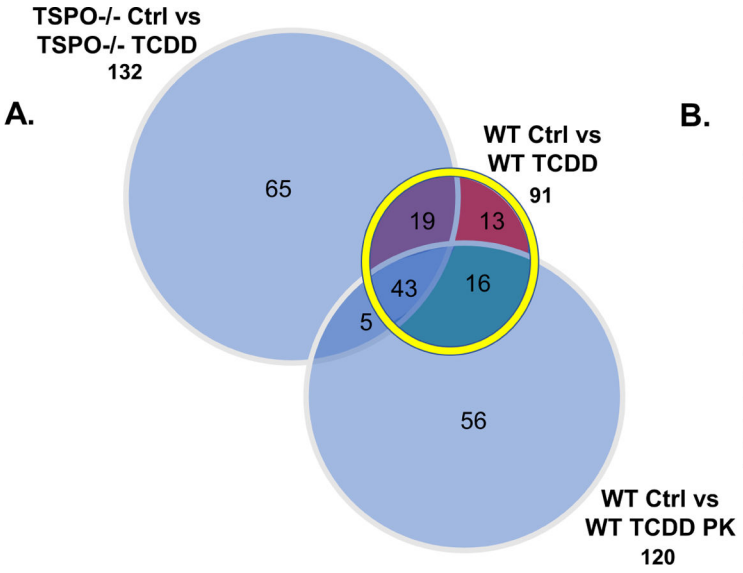

B.

name	Change	Gene description
Gm10358	-41.51	predicted gene 10358 GAPDH
Cacna1a	-1.25	calcium channel, voltage-dependent, P/Q type, alpha
Trp53bp2	-1.16	transformation related protein 53 binding protein 2
Flrt2	-1.15	fibronectin leucine rich transmembrane protein 2
Ahnak	1.19	AHNAK nucleoprotein (desmoyokin)
Gm28438	1.26	predicted gene 28438
Gm28437	1.36	predicted gene 28437
Lif	1.42	leukemia inhibitory factor
Arhgap45	1.65	Rho GTPase activating protein 45
Gsdme	1.67	gasdermin E
Dhrs3	1.90	dehydrogenase/reductase (SDR family) member 3
Padi1	2.20	peptidyl arginine deiminase, type I [Source:MGI
Gm22009	5.52	predicted gene, 22009 [Source:MGI

Fig. 5. Differentially expressed genes between control, TCDD-treated, or TCDD+PK11195-treated wild-type (WT) and TSPO−/− MLE-12 cells.

RNAseq was performed on wild type (WT) and TSPO−/− cells following treatment with TCDD or TCDD + PK11195 as described in materials and methods. Differentially expressed genes (padj < 0.05, n = 3) in the three groups were compared (**A**). There were 13 genes that were significantly changed following TCDD treatment in WT cells that were not significantly altered in the TSPO−/− cells following similar treatment nor in the WT cells following co-treatment with TCDD + PK11195 (**B**).

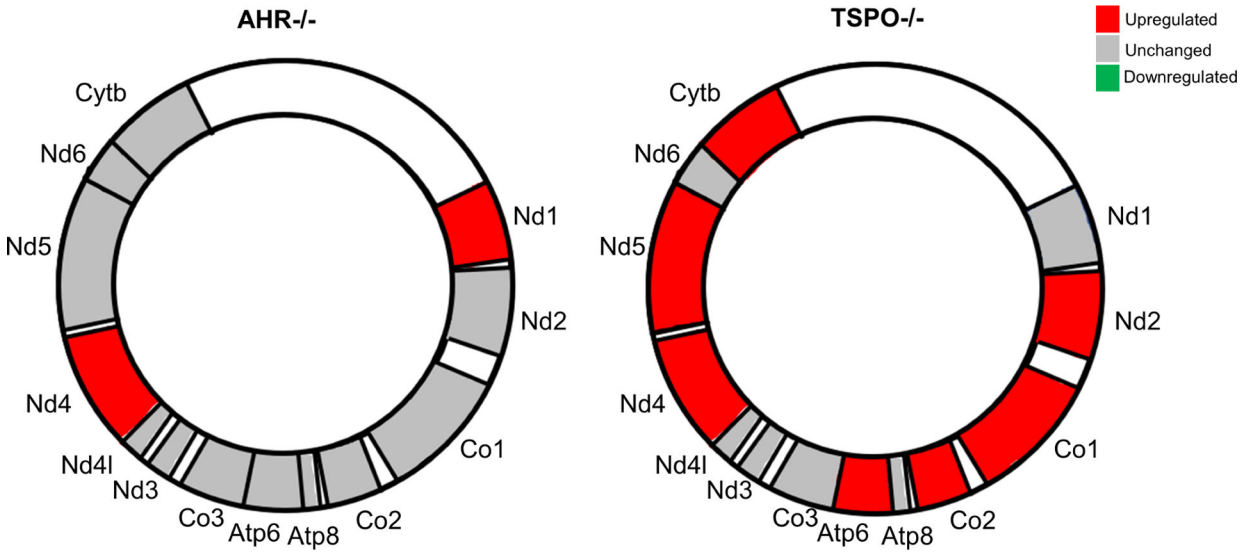

Fig. 6. Mitochondrial encoded genes were upregulated in AHR−/− and TSPO−/− MLE-12 cells.

Graphical representation of the 13 genes within the murine mitochondrial genome. RNA was isolated from untreated MLE-12 wild-type (WT), AHR−/−, and TSPO−/− cells using TRIzol protocol and sequenced by Novogene. Genes were designated as significantly upregulated or downregulated compared to WT if the padj < 0.05. n=3

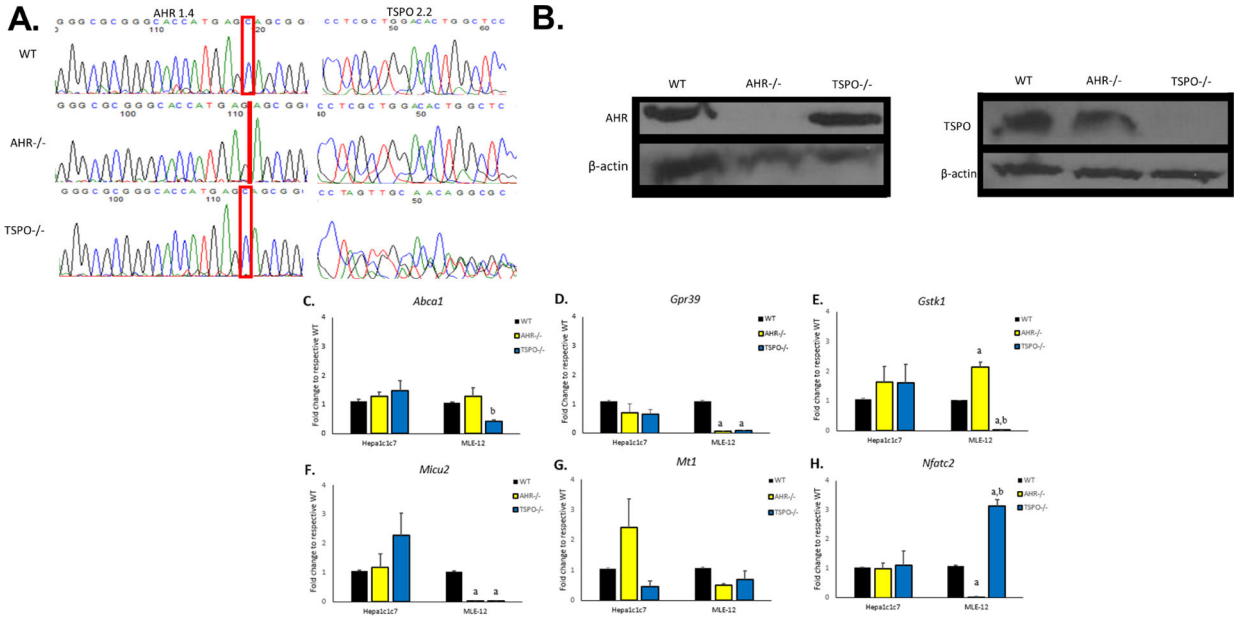

Fig. 7. Confirmation of AHR and TSPO CRISPR knockout in Hepa1c1c7 cells and comparison of select DEGs in Hepa1c1c7 and MLE-12.

Genomic DNA was extracted from 1c1c7 cells using Qiagen DNeasy Blood & Tissue Kit. CRISPR regions were amplified using specific primers and Q5 Polymerase PCR. PCR fragments were verified for size using gel electrophoresis and analyzed using Sanger Sequencing (**A**). Hepa1c1c7 were grown to exponential growth phase and then collected in RIPA buffer. Whole cell protein (37.5 μg for AHR and 150 μg for TSPO) was separated by SDS-PAGE and protein was transferred to nitrocellulose and probed for AHR, TSPO, or β-actin (loading control) (**B**) Hepa1c1c7 and MLE-12 cells were grown in 6 well dishes in triplicates, collected in TRIzol, and RNA isolated according to manufacturer's protocol. cDNA was created using GoScript Reverse Transcriptase per manufacter's protocol. qRT-PCR was performed using SYBR Green MasterMix. Gene expression was normalized using the geometric mean of housekeeping genes, *Hprt*, *Actb,* and *18s*, and calculated using $\Delta\Delta C_T$ method. Final comparisons were made as fold change to the wild-type control. a=significance from WT $p<0.05$. b=significance from AHR−/− $p<0.05$. (n=3) (**C-H**)

Table 1.

The impact of *Ahr* and *Tspo* knockout on the expression of five AHR target genes in MLE-12 cells.

	Wild Type			
	Control	**TCDD**	**PK11195**	**TCDD+PK**
Cyp1A1	0.0000	0.0943	0.0000	0.0471
Cyp1A2	0.0000	0.0288	0.0000	0.0000
Cyp1B1	43.6353	150.4421	45.3969	156.8090
AHRR	0.0016	0.0048	0.0000	0.0000
Nqo1	11.8222	25.3125	11.2235	24.6279
	AHR−/−			
	Control	**TCDD**	**PK11195**	**TCDD+PK**
Cyp1A1	0.0000	0.0000	0.0000	0.0000
Cyp1A2	0.0000	0.0233	0.0070	0.0000
Cyp1B1	40.8458	40.7283	40.2986	40.1564
AHRR	0.0015	0.0021	0.0000	0.0000
Nqo1	9.9061	10.0269	9.8448	9.6662
	TSPO−/−			
	Control	**TCDD**	**PK11195**	**TCDD+PK**
Cyp1A1	0.0000	0.5584	0.0000	0.5360
Cyp1A2	0.0000	0.0000	0.0000	0.0000
Cyp1B1	36.7047	216.0881	37.6043	218.0877
AHRR	0.0039	0.0000	0.0034	0.0121
Nqo1	11.0459	23.7388	11.0096	23.9986

Data were normalized and represented as fragments per kilobase per million mapped reads (fpkm). Green = padj < 0.05 compared to controls within the same cell type. Red = padj < 0.05 compared to control within cell type and compared to wild type cells within treatment.

Table 2.

Differential expression of mitochondrial calcium importer genes in CRISPR knockout AHR−/− and TSPO−/− MLE-12 cells.

	AHR−/−	TSPO−/−
Mcu	1.16	−1.28
Micu1	1.17	1.08
Micu2	−94.88	−94.08
Micu3	1.05	1.30
Smdt1	1.02	−1.06

Red= increase padj < 0.05 compared to WT, Green=decrease padj <0.05 compared to WT